J|A|C|S
ARTICLES

Interfacial Ion Transfers between a Monolayer Phase of Cationic Au Nanoparticles and Contacting Organic Solvent

Rajesh Sardar, Christopher A. Beasley, and Royce W. Murray*

Kenan Laboratories of Chemistry, University of North Carolina, Chapel Hill, North Carolina 27599

Received November 11, 2009; E-mail: rwm@email.unc.edu

Abstract: The highly cationic nanoparticle [Au_{225}(TEA-thiolate$^+$)$_{22}$(SC6Fc)$_9$] adsorbs so strongly on Pt electrodes from CH_3CN/Bu_4NClO_4 electrolyte solutions that films comprised of 1−2 monolayers of nanoparticles can be transferred to nanoparticle-free electrolyte solutions without desorption and ferrocene voltammetry stably observed. (TEA-thiolate$^+$ = -S(CH$_2$)$_{11}$N(CH$_2$CH$_3$)$_3$$^+$; SC6Fc = S(CH$_2$)$_6$-ferrocene; Fc = ferrocene). The Fc$^{+/0}$ redox couple's voltammetry is used to detect the adsorption. The apparent formal potential ($E^{\circ\prime}_{APP}$) of the Fc$^{+/0}$ couple depends on the electrolyte—its anion, cation, and concentration—in the contacting nanoparticle-free solution. A 10-fold change in electrolyte concentration shifts the Fc$^{+/0}$ $E^{\circ\prime}_{APP}$ by 48−67 mV, depending on the electrolyte. The dependency is interpreted to reflect the energetics of transfer of charge-compensating anions from the electrolyte solution to the monolayer nanoparticle "phase", promoted by the formation of Fc$^+$ sites in the nanoparticle film. This interpretation is supported by electrochemical quartz crystal microbalance results. Some further aspects of the results suggest adsorption of electrolyte cations at the nanoparticle film/electrolyte solution interface. The interface mimics a liquid/liquid interface between immiscible electrolyte solutions, in which the ion transfer approaches permselective behavior. The experimental results show that even 1−2 monolayers of highly ionic nanoparticles can behave as a polyelectrolyte "phase".

Introduction

Ion transfer at interfaces between immiscible electrolyte solutions (ITIES) has received considerable attention for fundamental reasons and because of its role in biological systems, phase transfer catalysis, and solar energy storage.[1−7] Interfacial displacement of charge generally corresponds to electrolyte ions moving across it, in response to a stimulus provided by charge-generating events—photonic or electrochemical—within the two electrolyte solutions.[8,9] The ion-transfer energetics involve $\Delta_{\text{soln}}^{\text{film}}\phi_{A}^{o\prime}$, the ion-transfer potential, meaning that a potential bias of that magnitude exists across the interface.

Herein we discuss the ion transfer between a 1−2 monolayer thick polyelectrolyte phase of highly cationic, ferrocene-labeled Au nanoparticles adsorbed on an electrode and a contacting electrolyte solution; the ion transfer occurs when the electrode potential is changed so as to initiate redox reactions of the ferrocene (Fc) sites. Since the working and reference electrodes lie on opposite sides of the nanoparticle film/solution interface, changes in the observed (apparent) Fc$^{+/0}$ formal potential ($E^{\circ\prime}_{APP}$) include the energetics of ion transfers across the interface, plus any actual changes in the Fc$^{+/0}$ formal potential provoked by associated alterations in ion and solvent population within the film. The observed potentials for ion transfers depend on electrolyte concentration, as generally expected for a permselective transfer of electrolyte anions into and out of the nanoparticle film. Electrolytes with different anions but identical cation display different $E^{\circ\prime}_{APP}$, reflecting differences in $\Delta_{\text{soln}}^{\text{film}}\phi_{A}^{o\prime}$. Unexpectedly, for a given electrolyte anion, shifts in the apparent $\Delta_{\text{soln}}^{\text{film}}\phi_{A}^{o\prime}$ also occur for different electrolyte cations. Our understanding of the nanoparticle film behavior is based on it acting as a "polyelectrolyte phase", even though only 1−2 monolayers thick.

The nanoparticles used are highly cationic (have quaternary ammonium groups) and are labeled with a small proportion of ferrocene groups to enable detection of the adsorption. The approximate *average* nanoparticle formula[10] is [Au_{225}(TEA-thiolate$^+$)$_{22}$(SC6Fc)$_9$], where TEA-thiolate$^+$ is -S(CH$_2$)$_{11}$-N(CH$_2$CH$_3$)$_3$$^+$ and SC6Fc = -S(CH$_2$)$_6$-ferrocene. This adsorption is analogous to previous observations where the thiolate ligand shell was fully ferrocenated.[11,12] Similar to the previous work,

---

(1) Girault, H. H.; Schiffrin, D. J. *Electrochemistry of Liquid−Liquid Interface*; Dekker: New York, 1989.
(2) Zhan, D.; Li, X.; Zhan, W.; Fan, F.-R, F.; Bard, A. J. *Anal. Chem.* **2007**, *79*, 5225–5231.
(3) Amemiya, S.; Yang, X.; Wazenegger, T. L. *J. Am. Chem. Soc.* **2003**, *125*, 11832–11833.
(4) Thompson, F. L.; Yellowlees, L. J.; Girault, H. H. *J. Chem. Soc., Chem. Commun.* **1988**, 1547.
(5) Flatte, M. E.; Kornyshev, A. A.; Urbakh, M. *Proc. Natl. Acad. Sci. U.S.A.* **2008**, *105*, 18212–18214.
(6) Shao, Y.; Stewart, A. A.; Girault, H. H. *J. Chem. Soc., Faraday Trans.* **1991**, *87*, 2593–2597.
(7) Yatziv, Y.; Turyan, I.; Mandler, D. *J. Am. Chem. Soc.* **2002**, *124*, 5618–5619.
(8) Kotov, N. A.; Kuzmin, M. G. *J. Electroanal. Chem.* **1990**, *285*, 223–240.
(9) Kotov, N. A.; Kuzmin, M. G. *J. Electroanal. Chem.* **1992**, *338*, 99–124.
(10) See the Experimental Section and Supporting Information.
(11) Wolfe, R. L.; Balasubramanian, R.; Tracy, J. B.; Murray, R. W. *Langmuir* **2007**, *23*, 2247–2254.
(12) Stiles, R. L.; Balasubramanian, B.; Feldberg, S. W.; Murray, R. W. *J. Am. Chem. Soc.* **2008**, *130*, 1856–1865.

10.1021/ja909584p

nanoparticle adsorption on the electrode is initiated by a cyclical potential scan through the $Fc^{+/0}$ wave in a CH_3CN/electrolyte solution containing dissolved nanoparticles, followed by washing of the Pt electrode and transfer to a fresh nanoparticle-free electrolyte solution. The adsorption is so strong that, even in the absence of dissolved nanoparticles, stable ferrocene voltammetry is observed, meaning that the nanoparticle film is tenaciously retained on the electrode surface. The adsorption coverage, as measured using the ferrocene redox label, amounts to 1−2 monolayers of nanoparticles. Such strong adsorption, in approximately monolayer quantities, nominally by solely electrostatic attachment to the electrode, is unusual, prompting our investigations[13] aimed at a better understanding of it. Our general interpretation is that nanoparticle adsorption is induced by specifically adsorbed electrolyte counterions and is entropically stabilized by formation of *multiple* interactions between adsorbed anions and cationic sites (e.g., quaternary ammonium and Fc^+) on the nanoparticle ligand shell. The stability is analogous to that of the chelate effect in metal complexes[14] and of "layer-by-layer" adsorption[15−17] of polyelectrolytes.

Scheme 1 illustrates our model of the adsorption, showing multiple ion-pair bridges between cationic nanoparticles and specifically electrode-adsorbed electrolyte anions. Further details on the nanoparticle adsorption will be presented in a subsequent publication.[18] The present report focuses on a phenomenon discovered in observing the formal potentials of the $Fc^{+/0}$ labels, namely that their *apparent* $E^{\circ\prime}_{APP}$ values vary with the electrolyte concentrations. We interpret these changes by considering that the approximate monolayer of adsorbed nanoparticles behaves as a polyelectrolyte "phase" and that the apparent redox potentials of the ferrocene labels are biased by the free energy of ions crossing the boundary of nanoparticle "phase" and CH_3CN electrolyte solution. The observed shifts in $E^{\circ\prime}_{APP}$ values are close to the ideal 59 mV per decade of electrolyte concentration expected for permselective ion transfers. They deviate from the ideal 59 mV, possibly owing to actual changes in the $Fc^{+/0}$ formal potential, provoked by the large changes in ion and solvent population within the film. Also, the ion transfer is ideally expected to involve only electrolyte anions, but the data show that the identity of the electrolyte cation matters. Electrochemical quartz crystal microbalance (EQCM) measurements suggest that concurrent solvent transfers also occur.

Our explanation of the changes in the apparent $E^{\circ\prime}_{APP}$ values of the $Fc^{+/0}$ couple is inspired by an interpretation by Quinn et al.[19,20] of aqueous electrolyte-induced shifts of formal potentials of one-electron nanoparticle core redox changes for monolayers of alkanethiolate-coated nanoparticles that were electrode-attached[21] (by bridging dithiolate ligands). The present work is the first investigation of the ion-transfer process for a highly ionic nanoparticle film, treating the nanoparticle monolayer as a polyelectrolyte "phase" and the energetics of counterions crossing the water/nanoparticle phase boundary as causing shifts in apparent formal potentials. The observations here differ from those by Quinn et al.[19,20] in several ways: (a) The changes in redox equivalents per nanoparticle (averaging nine in the present case) are much larger. The redox changes and associated ion (and solvent) transfers may provoke larger alterations in the monolayer "phase". (b) The solvent (CH_3CN) polarity is closer to that of the film. (c) The EQCM results demonstrate solvent accompanying ion transfer. (d) The nanoparticle "phase" resembles a polyelectrolye (the cation site concentration in a monolayer of $[Au_{225}(TEA\text{-}thiolate^+)_{22}(SC6Fc)_9]$ in the Fc^+ form is ca. 0.3 M).

Scheme 1. Redox-Labeled, Intrinsically Cationic, Nanoparticle Films Adsorbed on the Electrode Surface[a]

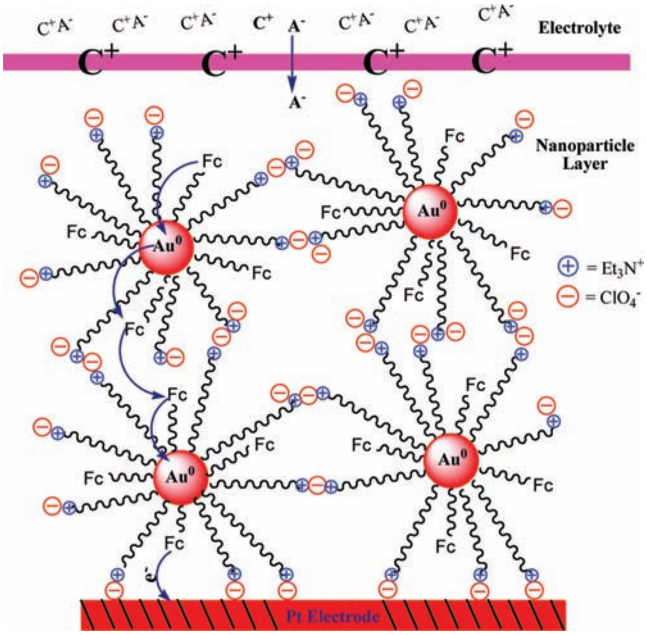

[a] The film is stable due to multiple ion-pair bridge interactions between adsorbed anions on the electrode surface and quaternary ammonium groups of the nanoparticle, possibly aided by ion-bridged interactions between nanoparticles laterally and vertically within the 1−2 monolayer thick nanoparticle film. During electrode potential scanning, the film undergoes $Fc^{+/0}$ redox changes in which charge compensation take place via transfer of anions from the contacting electrolyte solution to the nanoparticle film during ferrocene oxidation, and the reverse during reduction. The purple line indicates the film/solution interface where electrolyte cations are apparently adsorbed, biasing the electrolyte anion-transfer potential.

Experimental Section

Chemicals. 11-Bromo-1-undecene (>95%), triethylamine (NEt_3, >99%), thioacetic acid (>98%), *tert*-butylammonium borohydride (Bu_4NBH_4,>98%) *tert*-octylammonium bromide (Oct_4NBr, >98%), sodium borohydride ($NaBH_4$, >98%), *tert*-butylammonium perchlorate (Bu_4NClO_4, >99%), lithium perchlorate ($LiClO_4$, >98%), *tert*-butylammonium tetrafluoroborate (Bu_4NBF_4, >99%), *tert*-butylammonium hexafluorophosphate (Bu_4NPF_6, puress), and *tert*-ethylammonium perchlorate (Et_4NClO_4, >99%) from Aldrich and toluene (reagent grade), acetonitrile (Optima), methylene chloride (HPLC grade), tetrahydrofuran (HPLC grade), and ethanol (HPLC grade) from Fisher were used as received. $HAuCl_4 \cdot xH_2O$ (from

---

(13) Sardar, R.; Beasley, C. A.; Murray, R. W. *Anal. Chem.* **2009**, *81*, 6960–6965.

(14) (a) Busch, D. H. *Chem. Rev.* **1993**, *93*, 847–860. (b) Leininger, S.; Olenyuk, B.; Stang, P. J. *Chem. Rev.* **2000**, *100*, 853–908, and references therein.

(15) (a) Bertrand, P.; Jonas, A.; Laschewsky, A.; Legras, R. *Macromol. Rapid Commun.* **2000**, *21*, 319–348, and references therein. (b) Decher, G. *Science* **1997**, *277*, 1232–1237.

(16) Harris, J. J.; DeRose, P. M.; Bruening, M. L. *J. Am. Chem. Soc.* **1999**, *121*, 1978–1979.

(17) Xiao, K. P.; Harris, J. J.; Park, A.; Martin, C. M.; Pradeep, V.; Bruening, M. L. *Langmuir* **2001**, *17*, 8236–8241.

(18) Beasley, C. A.; Sardar, R.; Barnes, N. M.; Murray, R. W., unpublished results, UNC-Chapel Hill, 2009.

(19) Laaksonen, T.; Virginia, V.; Murtomaki, L.; Quinn, B. M. *J. Am. Chem. Soc.* **2007**, *129*, 7732–7733.

(20) Laaksonen, T.; Virginia, V.; Liljeroth, P.; Quinn, B. M. *J. Phys. Chem. C* **2008**, *112*, 15637–15642.

(21) Chen, S.; Pei, R. *J. Am. Chem. Soc.* **2001**, *123*, 10607–10615.

99.999% pure gold) was synthesized using a literature procedure[22] and stored in a freezer at −20 °C. Water was purified using a Barnstead NANOpure system (18 MΩ).

Synthesis of Ferrocene Hexanethiol and of *N,N,N*-Triethyl-(11-undecenylmercapto)ammonium Chloride (TEA-thiolate$^+$). Ferrocene hexanethiol (HSC6Fc) was synthesized as previously described;[11,23] the detailed procedure is provided in the Supporting Information. *N,N,N*-Triethyl(11-undecenylmercapto)ammonium chloride (TEA-thiolate$^+$) thiol, which has proved useful in nanoparticle mass spectrometry,[24] was synthesized via a modification of a previous report,[25] as described in the Supporting Information.

Synthesis of Quaternary Ammonium Thiolate Functionalized Monolayer-Protected Clusters (MPCs). The cationic thiolate-protected gold nanoparticles were synthesized via a modification of the Brust reaction.[26] The phase transfer agent, tetraoctylammonium bromide (3.0 g in 200 mL of toluene) was added to 1.37 g of $HAuCl_4$ in 100 mL of deionized water, and the mixture was stirred vigorously for 30 min, resulting in transfer of the Au salt to the (now orange-brown) organic phase. The quaternary ammonium-labeled thiol (2.0 g in 5 mL of ethanol) was added to the organic phase. The reaction mixture was stirred for 30 min at room temperature and then cooled to 0 °C in an ice bath, whereupon tetrabutylammonium borohydride (8.9 g in 50 mL of 9:1 toluene−ethanol at 0 °C) was quickly added. The reaction mixture immediately turned black, and after another 10 min of stirring a black solid started to precipitate. The mixture was stirred for another 20 min and then filtered using a fine glass frit, washed with a large excess of toluene followed by CH_2Cl_2, and dried under vacuum, yielding 0.89 g of nanoparticle product. Transmission electron microscopy (TEM) analysis (see the Supporting Information) of the TEA-thiolate$^+$ ligand-stabilized nanoparticles revealed an average diameter of 2.0 ± 0.3 nm, which is appropriate for an *average* formulation as a Au_{225} nanoparticle.[27] ^1H NMR analysis indicated an average of 31 thiolate ligands per nanoparticles, using ferrocene as an internal standard. The *average* nanoparticle composition is labeled as $Au_{225}(\text{TEA-thiolate}^+)_{31}$.

The nanoparticles were labeled by ferrocene using a ligand exchange between $Au_{225}(\text{TEA-thiolate}^+)_{31}$ and HSC6Fc (at a 1:1 ligand mole ratio). A mixture of 0.20 g of $Au_{225}(\text{TEA-thiolate}^+)_{31}$ and 0.042 g of HSC6Fc in 50 mL of ethanol was stirred for 4 h at room temperature. Addition of 0.10 g of $LiClO_4$ precipitated a black solid. The reaction mixture was stirred for 30 min, and then the solid was collected on a fine glass frit and washed with ethanol. The nanoparticle mixed monolayer *average* composition (by NMR) is $Au_{225}(\text{TEA-thiolate}^+)_{22}(\text{SC6Fc})_9$). It is presumed to be a perchlorate salt and is soluble in acetonitrile and dimethylformamide (DMF).

Electrochemistry. Voltammetry was done with a CH Instruments (Austin, TX) model 760C electrochemical analyzer. Solutions were typically degassed CH_3CN containing various electrolytes and concentrations, with either 0.05 mM $Au_{225}(\text{TEA-thiolate}^+)_{22}(\text{SC6Fc})_9$ or no nanoparticles. The electrolytes were ClO_4^-, PF_6^-, or BF_4^- salts of Bu_4N^+, and Li^+, Et_4N^+, or Hex_4N^+ salts of ClO_4^-. Electrodes were 1.6 mm diameter Pt disk working electrode, Pt wire counter electrode, and Ag/AgCl/3 M KCl(aq) reference electrode. Adsorption was induced by single cyclical potential scans (at 0.5 V/s from −0.1 to 1.0 V vs Ag/AgCl (aq)) in 1.0 M $Bu_4N^+ClO_4^-/CH_3CN$ containing the nanoparticle, followed by transfer at open circuit of the working electrode, with rinsing, to nanoparticle-free CH_3CN solutions of the same or some other electrolytes, at various concentrations. A 1-min equilibration of the nanoparticle film was allowed at each electrolyte concentration before the potential was scanned through the ferrocene wave, measuring its apparent formal potential ($E^{\circ\prime}_{APP}$, average of oxidation and reduction E_{PEAK}) and the nanoparticle surface coverage, Γ_{MPC} (mol/cm^2), from the charge under the ferrocene voltammetric peak,

$$Q = nA_mF\Gamma_{NP} \tag{1}$$

where n is the average number of ferrocenes per nanoparticle and A_m is the Pt working electrode area, corrected for a 2.8× roughness factor (as determined by hydrogen desorption voltammetry[28] in 0.10 M H_2SO_4). Experimental Γ_{MPC} values can be compared to an estimated model nanoparticle monolayer $\Gamma_{MONO} \approx 5.2 \times 10^{-12}$ mol MPC/cm^2 (assuming 32.2 nm^2 for $Au_{225}(\text{TEA-thiolate}^+)_{22}(\text{SC6Fc})_9$, based on overall particle radius *ca.* 3.2 nm). A reference electrode junction potential correction of 15 mV per decade of electrolyte concentration—obtained from voltammetry of ferrocene monomer in CH_3CN—was applied to apparent ferrocene formal potentials ($E^{\circ\prime}_{APP}$).

In some experiments, adsorption was induced in 1.0 M Bu_4NClO_4/CH_3CN, and then the electrode was rinsed with CH_3CN and transferred to a nanoparticle-free Bu_4NClO_4 electrolyte solution in a different solvent—e.g., CH_2Cl_2 or THF. We should mention that the nanoparticle adsorption occurs also with the immersed electrode at open circuit or held at a constant potential, and also occurs on other surfaces such as carbon, Au, and self-assembled monolayer (SAM)-functionalized (CO_2^-- and SO_3^--terminated SAMs)[13,18] Au electrodes.

QCM was performed (Stanford Res. Syst. QCM200, Sunnyvale, CA) on films deposited on 5 MHz AT-cut Au-quartz crystals by cycling the electrode potential between −0.1 and 1 V at 0.1 V/s in 0.025 mM nanoparticle/1 M Bu_4NClO_4/MeCN solution. The QCM holder and electrode were rinsed and transferred to 0.1 M Bu_4NClO_4/MeCN. Resolution was 0.1 Hz at a sampling time of 1 s, and electrochemistry was done with a CH Instruments CHI900a potentiostat (Austin, TX).

Results and Discussion

The experiments herein begin with the preparation of a stable, adherent film of nanoparticles with *average* formula $[Au_{225}(\text{TEA-thiolate}^+)_{22}(\text{SC6Fc})_9]$, where TEA-thiolate$^+$ = $S(CH_2)_{11}N(CH_2CH_3)_3^+$ and SC6Fc = $S(CH_2)_6$-ferrocene, by a single cyclical scan of the electrode potential in a solution of the nanoparticle in 1.0 M Bu_4NClO_4/CH_3CN electrolyte. The electrode is removed from this solution, rinsed, and transferred to a nanoparticle-free electrolyte solution—of selected electrolyte identity and concentration—where the voltammetry of the nanoparticle ferrocene labels (coverage and apparent ferrocene $E^{\circ\prime}_{APP}$ values) is observed.

Figure 1A shows voltammetry of the transferred adsorbed nanoparticle film where the transfer solution is 1.0 M $Bu_4N^+X^-$, where $X^- = PF_6^-$, ClO_4^-, or BF_4^- (as indicated) and the apparent $E^{\circ\prime}_{APP}$ values are 0.371, 0.388, or 0.409, respectively. Further, the observed $E^{\circ\prime}_{APP}$ values depend on the selected electrolyte concentration, as shown in Figure 1B. The apparent ferrocene formal potentials are linearly shifted by 52, 51, and 48 mV per decade of electrolyte concentration, respectively.

The electrode reaction in the above experiments can be written as

---

(22) Brauer, G. *Handbook of Preparative Inorganic Chemistry*; Academic Press: New York, 1965.

(23) Yu, C. J.; Wang, H.; Wan, Y. J.; Yowanto, H.; Kim, J. C.; Donilon, L. H.; Tao, C. L.; Strong, M.; Chong, Y. C. *J. Org. Chem.* **2001**, *66*, 2937–2942.

(24) Zinna-Fields, C. A.; Sardar, R.; Beasley, C. A.; Murray, R. W. *J. Am. Chem. Soc.* **2009**, *131*, 16266–16271.

(25) Tien, J.; Terfort, A.; Whitesides, G. M. *Langmuir* **1997**, *13*, 5349–5355.

(26) Brust, M.; Walker, M.; Bethell, D.; Schiffrin, D. J.; Whyman, R. *J. Chem. Soc., Chem. Commun.* **1994**, 801–802.

(27) Wolfe, R. L.; Murray, R. W. *Anal. Chem.* **2006**, *78*, 1167–1173.

(28) Bard, A. J.; Faulkner, L. R. *Electrochemical Methods*, 2nd ed.; Wiley: New York, 2001.

$$\mathrm{FcNP}^{n}_{\mathrm{film}} + \mathrm{X}^{-}_{\mathrm{soln}} \leftrightarrow \mathrm{FcNP}^{n+1}_{\mathrm{film}} + \mathrm{X}^{-}_{\mathrm{film}} + \mathrm{e}^{-} \qquad (2)$$

where the electrolyte anion is shown as entering the nanoparticle film to compensate the charge from electrogenerated ferrocenium sites (average nine per nanoparticle). The thermodynamics of the ion transfer,[29,30] as reflected in the observed apparent Fc^{0+} formal potential, $E^{\circ\prime}_{\mathrm{APP}}$, involves the actual $\mathrm{Fc}^{+/0}$ formal potential within the nanoparticle "phase", the standard ion-transfer potential $\Delta^{\mathrm{film}}_{\mathrm{soln}}\phi^{\mathrm{o}\prime}_{\mathrm{A}}$, the electrolyte concentration within the solution, and the concentration of ferrocene sites $[\mathrm{FcNP}]_{\mathrm{film}}$ within the film:[19]

$$E^{\mathrm{o}\prime}_{\mathrm{App}} = E^{\mathrm{o}\prime} + \Delta^{\mathrm{film}}_{\mathrm{soln}}\phi^{\mathrm{o}\prime}_{\mathrm{X}} + \frac{RT}{F}\ln\left(\frac{1}{2}[\mathrm{FcNP}]_{\mathrm{film}}\right) - \frac{RT}{F}\ln[\mathrm{X}^{-}_{\mathrm{soln}}] \qquad (3)$$

Since decay of the $\mathrm{Fc}^{+/0}$ wave during potential scanning is minimal (<3% over 25 cyclical scans, see the Supporting Information), $[\mathrm{FcNP}]_{\mathrm{film}}$ is taken as a constant during the experiments. The initial ferrocene charge state is taken as zero, and electrolyte cations are assumed to be excluded from the film by the Donnan exclusion principle.[31] This relation predicts that the apparent Fc^{0+} formal potential, $E^{\circ\prime}_{\mathrm{APP}}$, should shift by +59 mV per decade of decreasing electrolyte concentration, which is somewhat larger than the observed 48−52 mV shift. The *order* of the $E^{\circ\prime}_{\mathrm{APP}}$ values at 1.0 M electrolyte does mirror that of the ion-transfer potentials $\Delta^{\mathrm{film}}_{\mathrm{soln}}\phi^{\mathrm{o}\prime}_{\mathrm{X}}$ for these X^- anions observed[32,33] at water/dichlorobenzene interfaces, but the magnitudes of the differences between them are much smaller. Smaller differences in $\Delta^{\mathrm{film}}_{\mathrm{soln}}\phi^{\mathrm{o}\prime}_{\mathrm{X}}$ values are qualitatively expected because the polarity difference between the nanoparticle and $\mathrm{CH_3CN}$ phases is likely much less than that between water and dichlorobenzene (e.g., the nanoparticles are *soluble* in $\mathrm{CH_3CN}$). Thus, the ion-transfer behavior of the adsorbed $[\mathrm{Au}_{225}(\mathrm{TEA\text{-}thiolate}^{+})_{22}(\mathrm{SC6Fc})_{9}]$ "phase" is less ideal than that observed by Quinn et al.[19] for the very hydrophobic (water-insoluble) monolayer phase of alkanethiolate-coated Au nanoparticles contacted by an aqueous electrolyte.

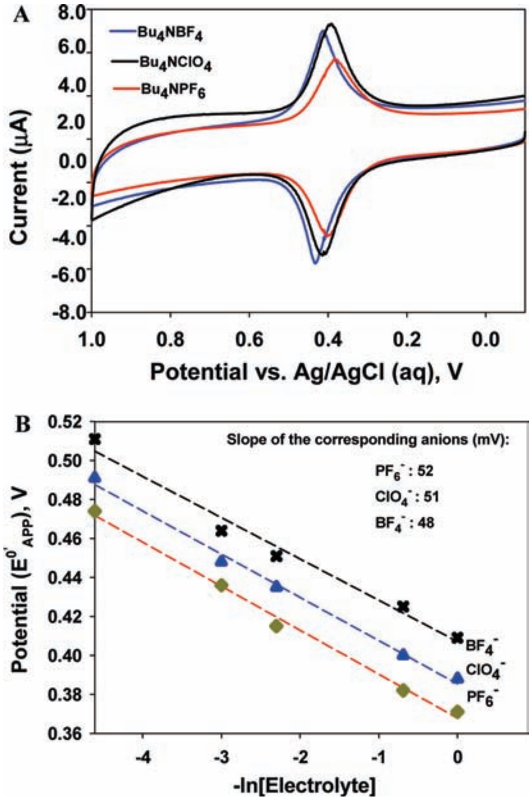

Figure 1. (A) Cyclic voltammetry of nanoparticles adsorbed on the electrode in different electrolytes; potential scan rate 0.5 V/s. The nanoparticle films had been prepared in 0.05 mM nanoparticle in 1.0 M $\mathrm{Bu_4NClO_4/CH_3CN}$ solutions and then transferred to 1.0 M nanoparticle-free $\mathrm{Bu_4N^+X^-/CH_3CN}$ solution, where $\mathrm{X} = \mathrm{BF_4^-}$, $\mathrm{ClO_4^-}$, or $\mathrm{PF_6^-}$. (B) Plot of apparent $\mathrm{Fc}^{+/0}$ formal potential, $E^{\circ\prime}_{\mathrm{APP}}$, against the electrolyte concentration in the nanoparticle-free $\mathrm{CH_3CN}$ solution to which the adsorbed films were transferred. The electrolytes were 1.0, 0.5, 0.1, 0.05, and 0.01 M $\mathrm{Bu_4N^+X^-/CH_3CN}$, where $\mathrm{X} = \mathrm{BF_4^-}$, $\mathrm{ClO_4^-}$, or $\mathrm{PF_6^-}$.

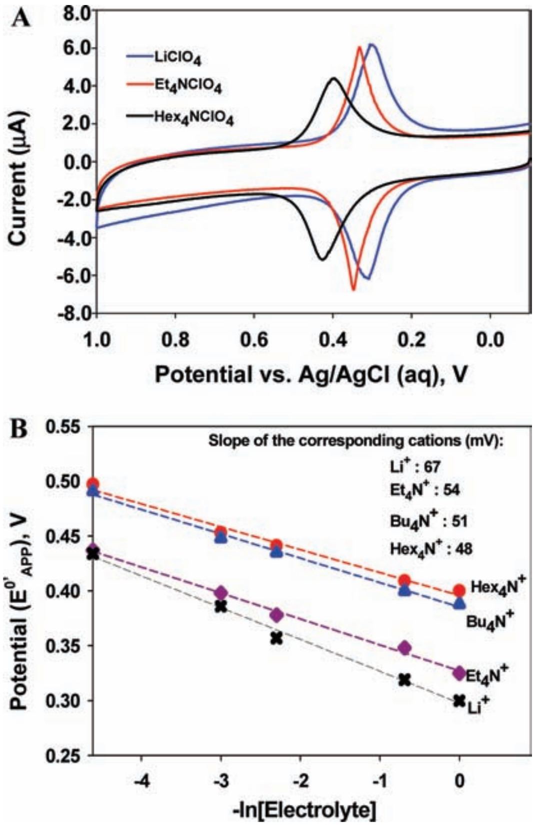

Figure 2. (A) Cyclic voltammetry of adsorbed nanoparticles on the electrode surface in different electrolytes with potential scan rate 0.5 V/s. The adsorbed nanoparticle films were prepared as 0.05 mM nanoparticle in 1.0 M $\mathrm{Bu_4NClO_4/CH_3CN}$ and transferred to 1.0 M nanoparticle-free $\mathrm{C^+ClO_4^-/CH_3CN}$ solution, where $\mathrm{C} = \mathrm{Li^+}$, $\mathrm{Et_4N^+}$, $\mathrm{Bu_4N^+}$ (CV is in Figure 1A), and $\mathrm{Hex_4N^+}$. (B) Plot of apparent $\mathrm{Fc}^{+/0}$ formal potential, $E^{\circ\prime}_{\mathrm{APP}}$, vs the concentration of electrolyte cation, $\mathrm{C^+}$, which was 1.0, 0.5, 0.1, 0.05, or 0.01 M $\mathrm{C^+ClO_4^-/CH_3CN}$ solution, where $\mathrm{C} = \mathrm{Li^+}$, $\mathrm{Et_4N^+}$, $\mathrm{Bu_4N^+}$, or $\mathrm{Hex_4N^+}$.

Another non-ideality is revealed by inspection of the behavior of the ferrocene $E^{\circ\prime}_{\mathrm{APP}}$ of the adsorbed nanoparticle film when transferred to perchlorate electrolytes having different cations. Figure 2A shows cyclic voltammetry of the transferred nanoparticle film in 1.0 M electrolyte/$\mathrm{CH_3CN}$ solutions where the cations are $\mathrm{Li^+}$, $\mathrm{Et_4N^+}$, $\mathrm{Bu_4N^+}$, and $\mathrm{Hex_4N^+}$. (The $\mathrm{Bu_4NClO_4}$

---

(29) Vanysek, P. *Electrochim. Acta* **1995**, *40*, 2481–2847.

(30) Su, B.; Nia, R. P.; Li, F.; Hojeij, M.; Prudent, M.; Corminboeuf, C.; Samec, Z.; Girault, H. H. *Angew. Chem., Int. Ed.* **2008**, *47*, 4675–4678.

(31) Vanysek, P.; Buck, R. P. *J. Electroanal. Chem.* **1991**, *297*, 19–35.

(32) Hundhammaer, B.; Muller, C.; Solomon, T.; Alemu, H.; Hassen, H. *J. Electroanal. Chem.* **1991**, *319*, 125–135.

(33) Volkov, A. G.; Deamer, D. W. *Liquid−Liquid Interface: Theory and Methods*; CRC Press, Inc.: Boca Raton, FL, 1996.

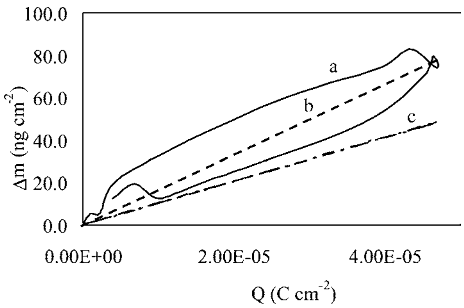

Figure 3. Gain of mass vs electrochemical charge response (a, —) during a cyclical potential scan (0.1 V/s) of an adsorbed [Au_{225}(TEA-thiolate$^+$)$_{22}$(SC6Fc)$_9$] film (where coverage $\Gamma_{NP} = 1.8 \times 10^{-11}$ mol/cm^2) in 0.1 M $LiClO_4/CH_3CN$. The overall slope (b, - - -) of the mass−charge response is 153 g/mol. The theoretical slope of the mass−charge response (c, − • −) assuming one ClO_4^- for each oxidation of ferrocene is 99.5 g mol^{-1}. The theoretical slope of the mass−charge response matches curve b if 1.2 mol of CH_3CN/mol of ClO_4^- enters the film upon ferrocene oxidation.

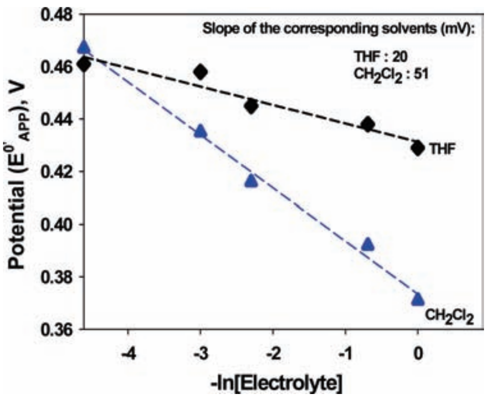

Figure 4. Plot of apparent $Fc^{+/0}$ formal potential $E^{\circ\prime}_{APP}$ vs the electrolyte concentration in different solvents. The adsorbed films were prepared from a 0.05 mM nanoparticle solution in 1.0 M Bu_4NClO_4/CH_3CN and then transferred to nanoparticle-free 1.0, 0.5, 0.1, 0.05, or 0.01 M Bu_4NClO_4/CH_2Cl_2 or Bu_4NClO_4/THF.

data are given in Figure 1.) The apparent formal potentials $E^{\circ\prime}_{APP}$ are 0.300, 0.325, 0.388, and 0.400 V vs Ag/AgCl(aq), respectively. Figure 2B shows that the $E^{\circ\prime}_{APP}$ values vary with the electrolyte concentration; the positive shifts are 67, 54, 51, and 48 mV per decade of concentration, respectively. Again, the electrolyte concentration dependencies show modest deviations from the ideal 59 mV expectation. The effect of the cation seems to be an augmentation of the anion's transfer potential value, $\Delta_{\mathrm{soln}}^{\mathrm{film}}\phi_{\mathrm{X}}^{\mathrm{o}\prime}$. Both this augmentation and the lower slopes (48−54 mV) for different electrolytes (in comparison to the ideal 59 mV per decade) in Figures 1B and 2B are interpreted as an effect of cation adsorption at the nanoparticle film/solution interface, as will be described later in the paper.

EQCM experiments were conducted to further explore the ion-transfer process for the nanoparticle "phase". An illustrative EQCM result is shown in Figure 3, for a cyclical potential scan of an adsorbed [Au_{225}(TEA-thiolate$^+$)$_{22}$(SC6Fc)$_9$] film transferred to 0.1 M $LiClO_4/CH_3CN$ electrolyte. The EQCM results are treated gravimetrically on the basis of the Sauerbrey equation, which assumes an acoustically thin, rigid film. The Figure 3 plot shows that the film gains mass (negative frequency shift) during the positive-going potential scan, and that the change in mass Δm is linear with the charge Q passed. The (mass change/mol charge) from the slope of the Figure 3 plot gives 153 g/mol. The prediction for transfer solely of ClO_4^- ions is smaller, 99 g/mol, but if allowance is made for concurrent solvent entry into the film, the experiment indicates that each ClO_4^- is accompanied by an average of 1.2 CH_3CN. Similar solvent transfer results have been reported in EQCM of electroactive polymer films,[34−36] and similar results are seen here for other electrolytes.

A few experiments were done to assess the influence of the solvent in the ion-transfer process. (All of the above were in CH_3CN.) If the prepared adsorbed nanoparticle film is transferred to an electrolyte solution in CH_2Cl_2 or in THF, results as shown in Figure 4 are obtained. The $E^{\circ\prime}_{APP}$ result in CH_2Cl_2, 51 mV per decade of electrolyte concentration, is very similar to that in CH_3CN (51 mV/decade), but that in THF solvent was only 20 mV/decade. The latter result reveals a serious loss in the ion-transfer selectivity in the case of THF solvent.

Concluding Remarks

Scheme 1 presents a model of the adsorbed nanoparticle film structure. The cationic nanoparticle is electrostatically bound to multiple specifically electrode-adsorbed electrolyte anions; the multiple bonding is the (entropic) origin of the strong and persistent nanoparticle adsorption. The scheme shows that one can consider that the voltammetric charging can involve the exit of electrolyte cations resident within the film and/or the entrance of charge-compensating anions from the contacting electrolyte solution. Perfect Donnan exclusion of co-ions from the strongly cationic nanoparticle "phase" would mean a negligible population of resident electrolyte cations exists within the film. The EQCM results are fully explainable by entry only of anions and nearly 1:1 solvent.

Given the preceding, it is striking that changing the electrolyte *cation* can displace the $E^{\circ\prime}_{APP}$ versus ln[electrolyte] plots of Figure 2B. As the hydrophobicity of the cation increases, the plots shift to substantially more positive $E^{\circ\prime}_{APP}$ values. Rather than ion transfer of a large population of electrolyte cations, we propose that the shifts in Figure 2B reflect an adsorption of these cations at the nanoparticle film/solution interface, where they artificially inflate the apparent values of the anion-transfer potential $\Delta_{\mathrm{soln}}^{\mathrm{film}}\phi_{\mathrm{X}}^{\mathrm{o}\prime}$. Further, a greater extent of interfacial adsorption at higher electrolyte concentration, by inflating $\Delta_{\mathrm{soln}}^{\mathrm{film}}\phi_{\mathrm{X}}^{\mathrm{o}\prime}$ more at high electrolyte concentration, would bias the $E^{\circ\prime}_{APP}$ versus ln[electrolyte] plot slopes toward lower values, as is seen in the Figure 2B series of perchlorates of Et_4N^+, Bu_4N^+, and Hex_4N^+, where the slopes are 54, 51, and 48 mV/decade. In this view, Li^+ does not adsorb at the film/solution interface, being a well-solvated ion in CH_3CN solvent.[37] Adsorption of species at liquid/liquid interfaces is well-known, and the effects of such adsorption can mimic changes in ion-transfer potentials.[38−40] By this interpretation, the interfacial adsorption of the

---

(34) Hillman, A. R.; Daisley, S. J.; Bruckenstein, S. *Electrochim. Acta* **2008**, *53*, 3763–3771.

(35) Jureviciute, I.; Bruckenstein, S.; Hillman, A. R. *Electrochim. Acta* **2006**, *51*, 2351–2357.

(36) Bruckenstein, S.; Jureviciute, I.; Hillman, A. R. *J. Electrochem. Soc.* **2003**, *150*, E285–E291.

(37) Marcus, Y. *Biophys. Chem.* **1994**, *51*, 111.

(38) Liu, B.; Mirkin, M. V. *J. Phys. Chem. B* **2002**, *106*, 3933–3940.

(39) Uchiyama, Y.; Kitamori, T.; Sawada, T. *Langmuir* **2000**, *16*, 6597–6600.

quaternary ammonium electrolyte cations can account for *both* the lower than ideal slopes of $E^{\circ\prime}_{\mathrm{APP}}$ versus ln[electrolyte] plots and their displacement from one another according to the cation identity (Figure 2B).

In summary, the process of ion transfer at the interface between CH_3CN electrolyte solutions and a film of adsorbed $[Au_{225}(TEA\text{-thiolate}^{+})_{22}(SC6Fc)_9]$ nanoparticles is more complex than that encountered by Quinn et al.[19] We believe these prior workers selected the correct physical model to account for shifts in nanoparticle potentials with electrolyte, but that in the present case other factors, notably the highly ionic nanoparticles and high cationic charge density inside the film phase, can play important roles in the ion-transfer process. The interface mimics a liquid/liquid interface between immiscible electrolyte solutions (ITIES), in which the ion transfer approaches permselective behavior. The experimental results show that even 1−2 monolayers of highly ionic nanoparticles can behave as a polyelectrolyte "phase".

Acknowledgment. This research was supported in part by grants from the Office of Naval Research and the National Science Foundation.

Supporting Information Available: Synthetic details, TEM characterization, supplementary coverage, and CV data. This material is available free of charge via the Internet at http://pubs.acs.org.

JA909584P

---

(40) Kakiuchi, T. *J. Electroanal. Chem.* **2001**, *496*, 137–142.